Proceedings of the 9th World Congress on Electrical Engineering and Computer Systems and Sciences (EECSS'23)
Brunel University, London, United Kingdom - August 03-05, 2023
Paper No. EEE 107
DOI: 10.11159/eee23.107

Control of Cascaded PV-Ćuk Converter Modules by Particle Swarm Optimization under Partial Shading Conditions

Mohamed Etarhouni[1], Benjamin Chong[2]
[1]International Study Centre/Liverpool John Moores University
L3 5UX, Liverpool, UK
M.S.ETARHOUNI@ljmu.ac.uk
[2]School of Electronic and Electrical Engineering/University of Leeds
LS2 9JT, Leeds, UK
ben.chong@leeds.ac.uk

Abstract - This paper presents a particle swarm optimization (PSO) technique for the maximum power point tracking of a PV power generation system under unequal solar irradiation. The system consists of multiple PV-Ćuk converter (PVCC) modules in a series chain and a terminal step-up converter for load connection. The bidirectional Ćuk converter in each PVCC has two PV panels connected at its four terminals. The configuration offers the advantage that under shading or module mismatching, the Ćuk converter provides a current bypass which can allow two PV panels track their available maximum power. The new PSO-based MPPT control scheme estimates the voltages corresponding to the maximum power each PV panel can generate under its specific weather conditions. Tuning of the controller parameters is based on the transfer function model of the proposed PVCC. The results show that the proposed PSO MPPT and model-based control can ensure high performance maximum power generation regardless of shading conditions.

Keywords**:** Cascaded PV-Ćuk converter (PVCC), Maximum power point estimating algorithm, Photovoltaic (PV) system, Partial shading, Particle swarm optimisation (PSO).

1. Introduction

The issue of partial shading in photovoltaic (PV) power generation systems has been well-investigated by many researchers [1-6]. A standard solution has involved incorporating bypass diodes within the PV array, but it has been recognized that this scheme alone reduces the power generated by the system [7-10].

Since the cost of power switching devices is steadily falling, the current trend is to replace the bypass diodes with power electronic converters, so that all series connected panels in an array can generate power corresponding to their respective levels of irradiation. Many such schemes have been proposed, based on either continuous or differential power processing approaches [10-14]. An example of the former is illustrated where one or several series and/or parallel chained PV panels are connected to a DC-DC converter forming a PV and converter integrated module [10]. Connecting multiples of such modules in series can raise the voltage levels sufficiently to enable transformer-less grid connection. Several well-known DC-DC converter topologies have been considered for such a scheme [10, 11]. However, the shortcomings of this scheme are twofold; firstly, the operating point of each of these modules is constantly changing in response to a system disturbance even though it may be, for example, due to the variation in light intensity level experienced by the other modules in the chain [12]. The other drawback is that the full power generated by each of these PV modules flows through their respective converters, causing additional power loss [10, 12].

The above shortcomings can be alleviated by using differential power processing scheme, which has been investigated by various researchers [10-14]. The two topologies used for such systems are bidirectional buck-boost converter (Fig.1 (a)) or Ćuk converter (Fig.1(b)) which are dual circuits. The Ćuk bidirectional converter uses capacitor C_n as energy storage component whereas the buck-boost type uses an inductor L_1. Both exhibit the same voltage transformation ratio for a given duty cycle k. The key advantage of these two forms is that under uniform solar irradiation, no PV generated power passes through the converters, and hence there is no converter power loss within the system. When partial shading occurs only a fraction of the power generated by its associated PV modules, according to the differences between the irradiation levels, is processed by the converter. Though there are still conversion losses in the terminal DC-DC converters, or DC-AC inverters for grid connection, the total power throughput should be higher than for the continuous scheme. Application of the buck-

boost converter for PV system was researched by [10, 11], The other architecture uses an isolated converter, such as a flyback type, to link each of the serially connected PV generators to the common DC bus output, forming the PV-to-bus architecture. Two main challenges exist for controlling this type of PV-to-PV architecture [10, 12]; firstly, adequate coordination of control schemes for PV DC-DC converters and terminal converter is needed to lead the system in achieving the maximum power point (MPP) operation. Secondly, minimizing the adverse effect to the converter dynamics due to the constantly changing PV operating points. In the authors' previous work, the first requirement was partly achieved by regulating the voltages of individual PV panels [11], and assuming the PV voltages at the MPPs are already known.

This paper presents a new particle swarm optimization (PSO) MPPT scheme for a PV generator formed by cascaded PV-Ćuk converter (PVCC) modules for panels under unequal lighting conditions. The preference for the Ćuk converter over the buck-boost topology is that the latter gives non-continuous input and output currents which requires large capacitors to shunt connect across the converter terminals or the PV modules. The proposed PSO-MPPT scheme for this PV power system estimates the MPP voltages for all the PV panels in the chain under their respective weather condition. A two-loop lead-lag control scheme is then used to determine the switching state and duty ratio for the Ćuk converters connected to each PVCC in the chain. The parameters of the controller are tuned based on the transfer function model of the PVCC, which is also detailed in the paper.

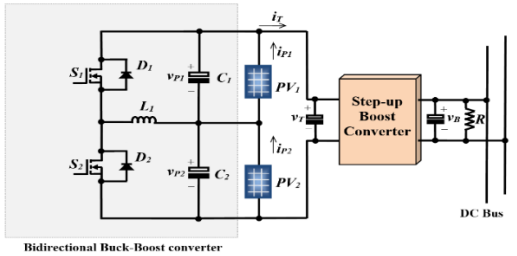

(a)

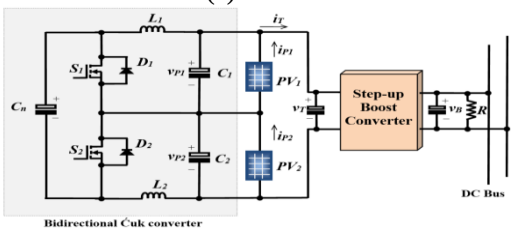

(b)

Fig. 1. Modules in Differential PV power processing system (a) bidirectional buck-boost converter (b) bidirectional Ćuk converter

2. Configuration of the Cascaded PVCC System

The system studied comprises multiple PVCC modules connected in series and a terminal step-up converter as shown in Fig.2. The circuit diagram of such a system with only a single PVCC module is shown in Fig.1(b). Each of the PVCC modules has a Ćuk bidirectional converter with its two terminal pairs connected to two serially linked PV panels (PV1 and PV2). Note that two adjacent PVCC modules are overlapped, namely they share one PV panel as shown in Fig.2. The advantage of using the Ćuk converter for two PV panels lies in its bidirectional feature, meaning that it can reverse the direction of both current and power flow. This is necessary since the two PV panels at its terminal pairs may have either sense of differential irradiation so the input and output sides of the converter must be interchangeable.

The operating principle of this system was explained in detail in the authors' previous paper [10]. To summarize, the inner Ćuk converter is used to establish the ratio between the voltages of two chained PV panels. The terminal boost converter is used for regulating the summed voltage of two series connected PV modules to reach the total MPP

voltage value. The key feature of this system lies in its two operating modes; one is when irradiation levels on two PV panels are the same. In this case the generated powers and currents from the PV panels are ideally the same, so the same current flows through the chained panels. Thus, with well-matched panels below some minimum threshold of illumination difference, the Ćuk converters which provide the current bypass path can be idled, giving infinitely high resistance along the path. For the second mode when the irradiations on the panels are different, i.e., the PV panels are partially shaded, their currents are different. The Ćuk converters are now required to provide a path for a portion of the PV current to flow. This can be done by regulating the two switch duty ratios of the Ćuk converter in the module, since it has the input and output voltage relationships given as [12]:

$$\frac{V_{PV2}}{V_{PV1}} = \frac{k_1}{1-k_1} \tag{1}$$

$$\frac{V_{PV1}}{V_{PV2}} = \frac{k_2}{1-k_2} \tag{2}$$

Where, V_{PV1} and V_{PV2} are, respectively, the terminal voltages of PV panels 1 and 2, k_1 and k_2 are duty ratios for switches S_1 and S_2 as shown in Fig.1 (b). Hence, Eq. (1) is used when the sunlight level on PV_1 module is higher than that of PV_2 and vice versa for Eq. (2).

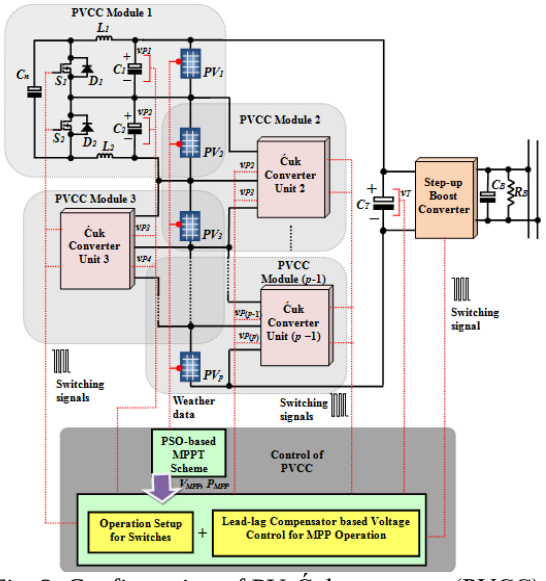

Fig. 2. Configuration of PV-Ćuk converter (PVCC) system

3. Particle Swarm Optimization (PSO)-based MPP Searching

The PSO-based MPPT algorithm enables all PV panels to operate at their respective MPP point even when their levels of solar irradiation are different. With the PV system having multiple chained PVCC modules as shown in Fig.2, the algorithm is applied simultaneously to estimate each of the PV panels voltages at their respective MPPs corresponding to their individual weather conditions. The PSO algorithm follows an iterative selection and result evaluation process. Starting from a random set of particles which are represented as voltages in this case, each may be a potential solution and has a fitness value evaluated using a fitness function. The objective of the algorithm is to find the optima by iteratively updating generations of particles. In detail, with a space containing N particles which are denoted as N positions, the velocities of updating respective particles and their positions at the m^{th} iteration are respectively denoted as v^m and x^m. All N new particle

position values, i.e., x^m, are then applied to a fitness function in turn and the one giving the best fitness value is denoted as the global best $(g_b)^m$. Also, after m iterations, each particle should have m updated values and the one giving the best fitness value is set as its best position $(p_b)^m$. In the next step $(m+1)$, the updated position of a particle is influenced by $(p_b)^m$ and the global best $(g_b)^m$. The velocity and particle position update formulas are written as follows:

$$v_b{}^{m+1} = \omega v_b{}^m + c_1 r_1[(p_b)^m - x_b{}^m] + c_2 r_2[(g_b)^m - x_b{}^m] \quad (3)$$

$$x_b{}^{m+1} = x_b{}^m + v_b{}^{m+1} \quad (4)$$

Where, ω is the inertia weight factor whose variation range can be defined by the user. c_1 and c_2 are the acceleration factors; r_1 and r_2 are random values lying between 0 and 1. To prevent the resultant particles moving out of range, their velocities and positions are limited to the ranges defined respectively by $[v_{min}, v_{max}]$ and $[x_{min}, x_{max}]$. The newly updated particle positions are then assessed using a fitness function and the process repeats.

When applying the above PSO algorithm to search for the MPP of a PV panel, the particles' positions are the PV terminal voltages, and each can be defined as $x = V_{pv}$. The fitness values of a random set of voltages are the output power which is evaluated using a simplified form of the original Bishop PV model [13]. The output power defines the fitness value for each particle which is evaluated as:

$$Fitness\ Function, f = I_{PV} V_{PV} \quad (5)$$

The flowchart for implementing this algorithm is shown in Fig. 3 and the procedures are listed below:

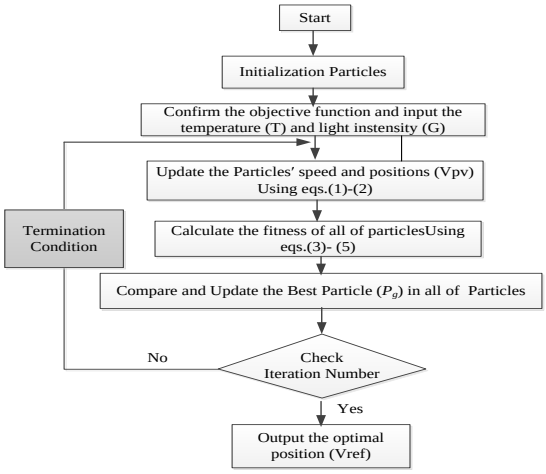

Fig. 3. Flowchart of the proposed MPPT method

4. Transfer Function Model of a PVCC Module

The estimated voltages from the PSO are then passed on to control the chained PVCC system. Each PVCC uses a lead-lag compensator whose parameters rely on accurate knowledge of the PV- Ćuk converter characteristics, thus a transfer function model for a PVCC module shown in Fig.2 needs to be derived. For a PVCC module, the state vector $\boldsymbol{x} = [i_{L1} \quad i_{L2} \quad v_{P1} \quad v_{P2} \quad v_{cn}]^T$ consists of instantaneous voltages and currents of the converters. Two state space equations for the converter, one for S_1 on state and the other for S_1 off state, can be written. Combining these two equations leads to a simplified overall average equation for one switching period, T_p. The converter's passive components are chosen such that $L_1 = L_2$ and $C_1 = C_2$. The terminal boost converter shown in Fig.1 is used to deliver the total generated power to the load and/or to a DC-bus. The power rating of the boost converter should be, at least,

equal to the sum of all chained PV panels and has much slower dynamics than any of the PVCC module voltage across PV_1 as the controlled variable, the transfer function between them is written as

$$G_{v1}(s) = \frac{\Delta v_{P1}(s)}{\Delta k_1(s)} = \boldsymbol{Z_1}(s\boldsymbol{I} - \boldsymbol{A}^*_{sm})\boldsymbol{J} = -\frac{\beta_3 s^3+\beta_2 s^2+\beta_1 s+\beta_0}{\alpha_5 s^5+\alpha_4 s^4+\alpha_3 s^3+\alpha_2 s^2+\alpha_1 s+\alpha_0} V_T \quad (6)$$

Table 1: Experimental Circuit Parameters.

Ćuk Converter $L_1 = L_2$	2.2mH
Ćuk Converter $C_1 = C_2$	22μF
Ćuk Converter C_n	82μF
Terminal Capacitor C_T	470μF
Switching Devices	MOSFETs: STB24NF1
Switching Frequency	20kHz
Load Resistance	35.Ω

4.1. Experimental Validation of the Model

The above transfer function model has been validated using an experimental set-up having two identical PV panels (Sunsei SE-6000) connected on two terminals of a bidirectional Ćuk converter [13]. The photographs of PV panels with the converter under two identical in-house built controllable sun light simulators are given in Fig.4 (a) and (b). The light level for each sun-simulator can be varied from zero to its maximum value (i.e., 0 to 100%) which corresponds to a solar irradiation of 0.505 kW/m^2. The parameters of the converters in the experimental set-up are given in Table 1.

The experiments were performed by setting the irradiation levels of the two solar simulators to give 100% for PV_1 and 40% for PV_2. The corresponding I-V curves measured from these two panels are shown in Fig. 4(c).

(a) (b) (c)

Fig. 4. Experimental setup: (a) PV panels and solar simulator system, (b) Cuk converter circuit for one PVCC module and (c) I-V characteristics for the PV panel under different light levels.

For all these cases, the voltage variation range is from 12-18 V.

5. Model-Based Control of a Chained PVCC System

The above validated model is then applied to tune the parameters of the voltage lead-lag compensators for controlling the chained PVCC as shown in Fig.1. The requirements for the controller are that the tracking of MPP voltages to be fast and accurate with the minimum fluctuation when a sudden change of weather condition occurs. With multiple PVCCs in a

chain, coordinated control is required for both the inner bidirectional Ćuk and terminal Boost converters. This can be used to determine the active switch pair in each PVCC module as follows:
1) Obtain the P_{MPPn} (n=*1, 2, …*) and corresponding V_{MPPn} for all PV panels in the chain from the PSO-based maximum power tracking scheme.
2) Estimate all the PV currents I_{Pn} using the obtained P_{MPPn} and V_{MPPn} and the desirable M_j terms (i.e., M_1, M_2, …, M_j, …, $M_{(p-1)}$). Note that M_j is the ratio between the j^{th} and $(j+1)^{th}$ PV panels respective maximum power voltages.
3) Evaluate the first PVCC converter current as $I_{L11} = I_{P1} - I_T$ where terminal current can be evaluated by using the sum of total P panels' maximum powers divided by the sum of their voltages at MPPs.
4) Iteratively evaluate I_{L1j} for j = 2, 3, …., p-1.
5) If $I_{L1j} > 0$, S_1-D_2 device pair in the j^{th} PVCC module is activated, otherwise $S_2 - D_1$ pair in this module is activated.

5.1. Voltage Feedback control of Ćuk Converters

Once the active switch pair in the Ćuk Converter of each PVCC is chosen, a two-loop control scheme is applied, instead of using a two-input-two-output control scheme. This is because that each PVCC, once its switching pair is determined, is a uni-directional converter, i.e., one PV voltage connected to the converter can be assumed the input source and maintained constant, the other is the controllable output. Though the input end voltage may vary due to the changes of adjacent unit, such variations can be considered disturbances and can be eliminated. Following the two-loop control, the duty ratio the converter is firstly determined according to the two PV voltages to follow the PSO predicted maximum power values. As shown in Fig. 5, there is a main loop and a detuning loop $H_i(s)$ (i=1,2) for j^{th} PVCC, if the active switch pair is S_2-D_1 for the j^{th} PVCC unit, so j^{th} PV panel voltage is controlled in the main loop, while the $(j+1)^{th}$ PV voltage is maintained by detuning the control signal from the main loop. The controllers are lead-lag compensators, and their parameters are tuned according to the derived transfer function model.

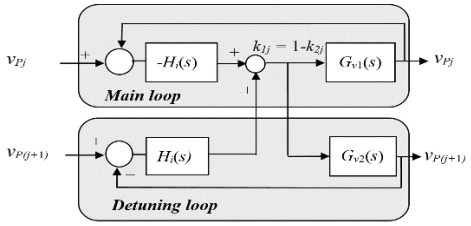

Fig. 5. Two loop control schemes for controlling the PV array terminal voltages

6. Experimental, Simulation Results & Discussions

The above control scheme was applied to a MATLAB-SIMULINK simulated PV system consisting of two PVCC modules as shown in Fig. 1(b). This has three nominally identical PV panels (i.e., PV_1, PV_2 and PV_3); PVCC module 1 is connected between PV_1 and PV_2 while PVCC module 2 between PV_2 and PV_3. Note that the L_B is the essential energy storage element for the terminal step-up converter. Its value is determined for desired current ripple $\Delta I/I_L$ to be about 5%, the switching frequency is 5 kHz and k being 0.5. In addition, the basic parameters used in the PSO-MPPT are set as: inertia weight ω = 0.5, acceleration factors c_1=c_2=2, maximum iterative number of PSO=50, and number of particles=20. Three different light irradiation conditions are set as shown in Fig. 6.

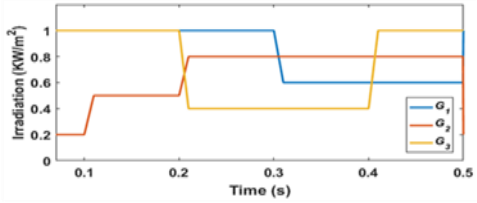

Fig. 6. Solar radiation variation in the system simulation.

The transient responses of these tests are measured as presented in Fig.7 (a). For comparison the parameters of the derived transfer function model derived are set to the same values as those listed in Table 1 and the model is implemented using MATLAB by varying duty ratio in the same way as the experimental test. The transient responses of the model for all four cases are shown in Fig. 7(b), thus, Fig.7 (c)depicts power output curves. Clearly all model response curves agree well with their corresponding experimental results.

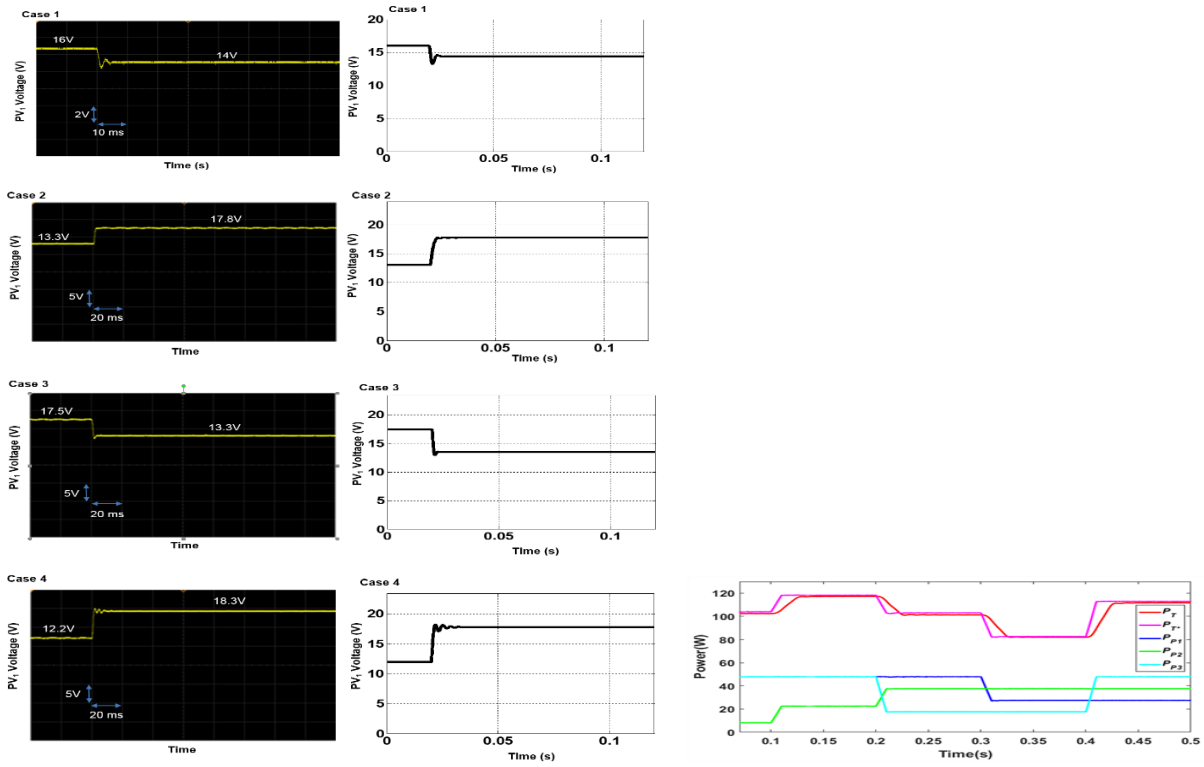

(a) (b) (c)

Fig. 7. Dynamical model verification for PVCC (a) Experimental step responses (b) Simulated step responses, and (c) Simulated average power for each PV module and the total power delivered to the load.

Detail explanations are summarized below:

1. From $t = 0$ to $t = 0.2$ s, PV_2 always receives the least solar irradiation while PV_1 and PV_3 are equally irradiated. The PSO-MPP tracking scheme estimates the maximum PV powers of each panel and their corresponding voltages while according to switch pair setup, S_1-D_2 of PVCC1 and S_2 -D_1 of PVCC2 should be activated. This prompts both lead-lag compensators for the inner Ćuks and the P+I controller of the terminal boost converter to regulate the duty ratios until the MPP voltages are reached. Following a step change in G_2 around $t = 0.1$ s, the voltage in PV_2 takes 0.03 s to reach the new MPP operating voltage. The voltages across PV_1 and PV_3 are disturbed and take about 0.04 s to recover to their original states.
2. From $t = 0.2$ to $t = 0.5$ s, all PV panels receive different solar irradiations throughout the period. At $t = 0.2$ s active switch pair for PVCC1 is still S_1-D_2 but for PVCC2 its S_1-D_2 becomes active since $G_2 > G_3$. Both V_{PV2} and V_{PV3} are controlled to their MPP values while V_{PV1} is maintained to its original value for MPP generation after a small disturbance.
3. At $t = 0.3$ s, G_1 reduces to below G_2, while G_2 and G_3 are unchanged. V_{PV1} is regulated to the value estimated by PSO algorithm as expected, but both V_{PV2} and V_{PV3} are maintained to their respective MPP values despite small disturbances.
4. Similarly, when G_3 has a step increase at $t = 0.4$ s, active switch pair in PVCC2 becomes S_1-D_2, while that in PVCC1 is unchanged. V_{PV3} is controlled to its desired level in about 0.05 S but V_{PV1} and V_{PV2} maintain their original values even though

they are disturbed due to operation point changes. The variations of corresponding terminal voltage V_T. As can be seen, V_T is always equal to the sum of all three PV panels' MPP voltages under all light intensities.

7. Conclusion

The paper presented a PSO-based maximum power point estimation algorithm applied to a PV- Ćuk converter system to enable all PV panels' maximum power voltages according to their weather conditions. The PV-converter integrated system consists of multiple PV-Ćuk converter modules connected in a series chain with a terminal step-up converter for load connection. The PSO estimated MPP voltages were used as the reference values in the two-loop feedback control scheme for each PVCC module in a system. The simulation study performed on the PV system formed by two PVCC modules and three PV panels has shown that the terminal voltages of all PV panels can track closely to the PSO predicted MPP voltages with accuracy and minimum oscillation. The total voltage of the whole system, i.e., the input voltage of the terminal boost converter has been shown to be the sum of the individual PV panel's MPP voltages, and the total power is the sum of the individual powers under all three different irradiation levels.

References

[1]. Dhanalakshmi, B. and N. Rajasekar, A novel Competence Square based PV array reconfiguration technique for solar PV maximum power extraction. Energy Conversion and Management, 2018. 174: p. 897-912.

[2]. Venkateswari, R. and N. Rajasekar, Power enhancement of PV system via physical array reconfiguration-based Lo Shu technique. Energy Conversion and Management, 2020. 215: p. 112885.

[3]. Manjunath, H.N. Suresh, and S. Rajanna, Performance enhancement of Hybrid interconnected Solar Photovoltaic array using shade dispersion Magic Square Puzzle Pattern technique under partial shading conditions. Solar Energy, 2019. 194: p. 602-617.

[4]. Meerimatha, G. and B.L. Rao, Novel reconfiguration approach to reduce line losses of the photovoltaic array under various shading conditions. Energy, 2020. 196: p. 117120.

[5]. Agrawal, N., B. Bora, and A. Kapoor, Experimental investigations of fault tolerance due to shading in photovoltaic modules with different interconnected solar cell networks. Solar Energy, 2020. 211: p. 1239-1254.

[6]. Tatabhatla, V.M.R., A. Agarwal, and T. Kanumuri, Improved power generation by dispersing the uniform and non-uniform partial shades in solar photovoltaic array. Energy Conversion and Management, 2019. 197: p. 111825.

[7]. Satpathy, P.R. and R. Sharma, Parametric indicators for partial shading and fault prediction in photovoltaic arrays with various interconnection topologies. Energy Conversion and Management, 2020. 219: p. 113018.

[8]. G.S. Krishna, T. Moger, Enhancement of maximum power output through reconfiguration techniques under non-uniform irradiance conditions, Energy 187 (2019), 115917.

[9]. H. Rezk, A. Fathy, M. Aly, A robust photovoltaic array reconfiguration strategy based on coyote optimization algorithm for enhancing the extracted power under partial shadow condition, Energy Rep. 7 (2021) 109–124.

[10]. M. Etarhouni, B. Chong, and L. Zhang, "A Combined Scheme for Maximising the Output Power of a Photovoltaic Array under Partial Shading Conditions". Sustainable Energy Technologies and Assessments Journal, Elsevier, DOI: 10.1016/j.seta.2021.101878.

[11]. Lee, H. and K. Kim, *Design Considerations for Parallel Differential Power Processing Converters in a Photovoltaic-Powered Wearable Application.* Energies, 2018. **11**: p. 3329.

[12]. Chong, B.V.P. and L. Zhang, *Controller design for integrated PV–converter modules under partial shading conditions.* Solar Energy, 2013. **92**: p. 123-138.

[13]. Ishaque, K. and Z. Salam, *A Deterministic Particle Swarm Optimization Maximum Power Point Tracker for Photovoltaic System Under Partial Shading Condition.* IEEE Transactions on Industrial Electronics, 2013. **60**(8): p. 3195-3206.

[14]. Ram, J.P. and N. Rajasekar, *A Novel Flower Pollination Based Global Maximum Power Point Method for Solar Maximum Power Point Tracking.* IEEE Transactions on Power Electronics, 2017. **32**(11): p. 8486-8499.